

Figure 1. Relationship between number average molecular weight and thickness of polymer brushes. $\langle S^2 \rangle^{1/2}_{\text{PMMA}}$ is the calculated mean-square radius of gyration of atactic PMMA in acetonitrile at 317 K.¹⁶

nm). The thickness of a densely grafted polymer brush increases linearly with the M_n of the grafted polymer. From a linear relationship between the thickness (L_d) and M_n of the tethered polymers, graft density σ was estimated to be about 0.61 chains/nm², which is higher than that of PMMA (ca. 0.47 chains/nm²), according to the following equation:

$$\delta = \frac{d \cdot L_d \cdot N_A \cdot 10^{-21}}{M_n}$$

where d and N_A are the density of polymers at 293 K and Avogadro's number, respectively. Chain dimensions of atactic PMMA chains with random coil conformation, which is calculated from root-mean-square radius of gyration ($2\langle S^2 \rangle^{1/2}$) in θ state (acetonitrile solution, 317 K), are also shown in Figure 1. The PMBL and PMMA brushes have a thickness higher than random coil dimension but lower than all trans extended-chain conformation, which indicates that a densely packed brush layer has formed and the chain conformation has been stretched almost perpendicular to the substrate. Simultaneous growth of PMBL chains from the substrate through controlled radical polymerization affords a high-density polymer brush. Due to the cyclic side group, PMBL has a density (d) 1.14 times higher than that of PMMA, which also contributes to the high graft density. For the PMBL brushes, there was no deviation from the proportional relationship at high molecular weight.

Scanning force microscopy revealed that a homogeneous PMBL layer was formed on the substrate. The root-mean-square (rms) surface roughness was less than 1.0 nm in dry state over a $20 \times 20 \mu\text{m}^2$ scanning area (Figure S1, Supporting Information). As reference, spin-coated PMBL samples were prepared from trifluoroethanol solution on a silicon wafer. The surface geometry of the spin-coated films was inhomogeneous, with rms surface roughness greater than 50 nm. Poor solubility and poor ductility prevent the formation of a smooth surface through the spin-casting procedure. X-ray photoelectron spectroscopy of the PMBL brushes revealed a large decrease in silicon peak intensity and an increase in oxygen and carbon peaks, which indicates that the surface is covered with thick PMBL brushes. The formation of the PMBL brushes was also verified by IR spectroscopy. IR spectroscopic measurements were made in the Brewster's angle configuration, where a p -

polarized IR beam incident to the surface at the Brewster's angle ($\theta = 73.7^\circ$ for an Si refractive index of 3.42). This approach is a powerful tool for obtaining high-resolution IR spectra of thin organic layers on a Si wafer in direct transmission mode.⁹ The IR spectra of the PMBL brushes exhibited an absorption peak corresponding to the stretching vibration of carbonyl groups in PMBL chains.

The elastic moduli of the polymer brushes and spin-coated films were obtained from force-curve measurements using scanning force microscopy. The results are presented as relative magnitudes of moduli because of the dependence of tip-shape, spring constant, and radius of curvature of the cantilever on absolute magnitude. The Hertzian contact model was applied to describe the tip penetration depth into the surface.^{7,10} This approximation neglects adhesive interaction between the probe and sample, as well as the viscous response of the polymer. A sphere-tip cantilever with relatively high spring constant (42 N/m) and large radius of curvature (400 nm) was used. After each measurement, additional reference force curves were taken on a silicon wafer to ensure that the calibration remained constant throughout the experiment. Over 100 force-curves were collected to obtain a statistical average of relative elastic modulus, which are shown in Figure 2. In both PMMA and

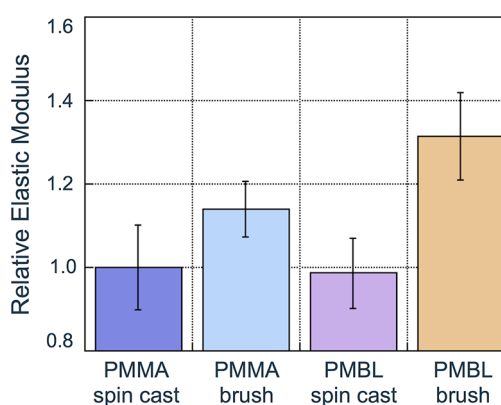
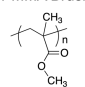
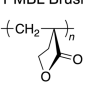


Figure 2. Relative magnitude of elastic moduli of spin-coated films and polymer brushes of PMMA and PMBL. The thickness of PMMA brush and PMBL brush is 61.7 and 66.4 nm, respectively. The thickness of the spin-coated films is over 100 nm.

PMBL, the polymer brushes exhibit higher elastic modulus than the respective spin-coated films. The increased modulus is attributed to the highly stretched conformation of the polymer brushes perpendicular to the substrate. The relative elastic modulus of the PMBL brushes was about 1.3 times higher than that of the PMMA brushes.

Dynamic contact angles of water on the polymer brushes were measured by expansion-shrinkage method.¹¹ The PMBL brushes exhibit much lower contact angles and high hysteresis with respect to the PMMA brushes, as listed in Table 1. Therefore, the PMBL brush surface is more hydrophilic than the PMMA brush surface. Intermolecular interaction can be estimated by a surface free energy of solids and it can be resolved into contribution from dispersion and dipole-hydrogen bonding forces. Surface free energy of the polymer brushes was calculated using the Owens–Wendt equation with static contact angle measurement results of water and ethylene glycol.¹² The surface free energy of the PMBL brushes and PMMA brushes was estimated to be 42 and 33 mN/m, respectively. The PMBL brushes have higher surface free

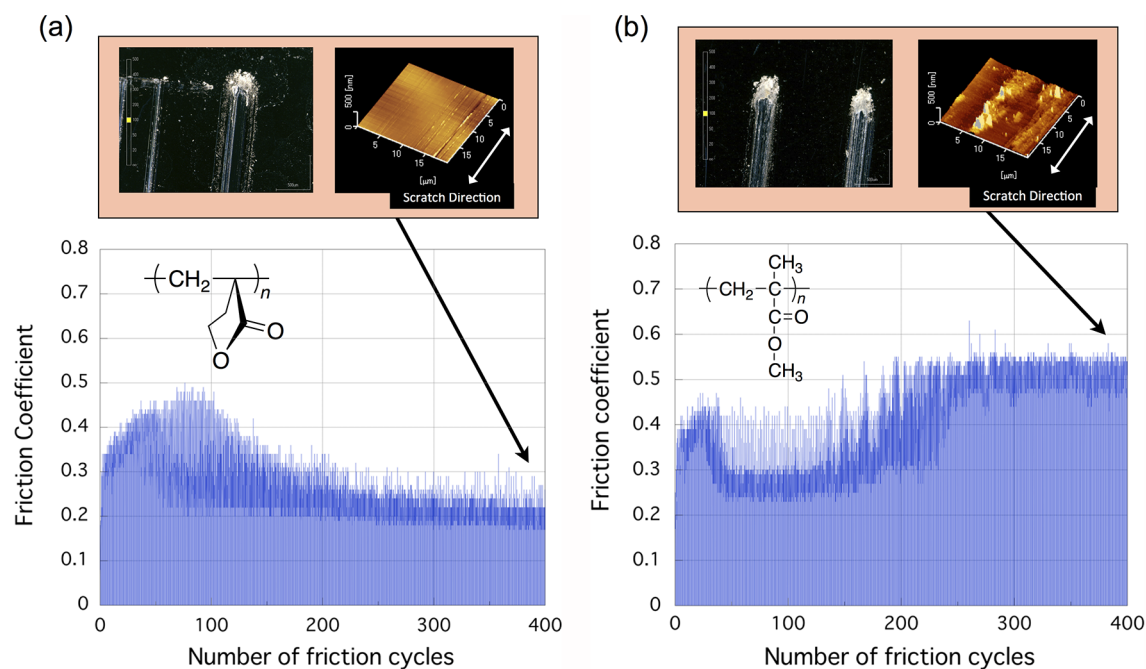
Table 1. Contact Angles and Surface Free Energy for PMBL and PMMA Brushes

	Static Contact Angle (°)				Surface Free Energy (mJ/m ²)	
	Water			Ethylene Glycol	γ _s ^d	γ _s ^p
	θ _S	θ _A	θ _R	θ _S		
PMMA Brush 	72 ± 1.3	76 ± 1.5	57 ± 1.4	50 ± 1.2	17	16
PMBL Brush 	59 ± 1.1	60 ± 2.6	24 ± 1.9	41 ± 1.1	12	30

energy than PMMA brushes. The polar component of PMBL is higher than PMMA because of the absence of α -methyl group and the higher density. This indicates that the increase in elastic modulus may be attributed to both the densely packed, stretched conformation and polar interactions between PMBL chains. Polar interactions between the PMBL brush chains lead to greater cooperative motion as well as a more rigid structure. It is clear that the surface roughness of the polymer brushes does not influence the magnitude of contact angle, because the root-mean-square surface roughness of both brushes is less than 1.0 nm. Because PMBL thin films with smooth surface cannot be prepared through spin-coated method; therefore, dynamic and static contact angle measurements were carried out only on brush films with smooth surface.

Macroscopic friction tests on the polymer brushes were carried out using a Tribostation Type32 (Shinto Scientific Co. Ltd., Tokyo), which is a conventional ball-on-plate type reciprocating tribometer. Measurements were made by sliding a stainless steel ball on the substrate at a reciprocating distance of 20 mm and with friction rate of $1.5 \times 10^{-3} \text{ ms}^{-1}$ in a dry nitrogen atmosphere under normal load of 0.49 N at room temperature. The theoretical contact area between the stainless

steel probe and substrate was estimated to be $2.44 \times 10^{-9} \text{ m}^2$ based on Hertzian contact mechanics theory. The average pressure on the contact area was estimated to be 200 MPa.¹³ It has been previously shown that the wear resistance of PMMA brushes is superior to their spin-coated counterpart.⁷ The high-density anisotropic brush chains restrict the mobility of the tethered polymer chains, which raises the effective glass transition temperature and elastic modulus.¹⁴ The high elastic modulus narrows the contact area to reduce the effective adhesive forces. In this work, we have sought to improve the wear resistance by appropriate control of molecular structure. The variation of friction coefficient of polymer brushes is shown in Figure 3 as a function of number of friction cycles. The friction coefficient of the PMMA brush films gradually increases, and exceeds 0.5 after about 200 tracking cycles. A significant amount of wear debris was observed at the edge of the wear track. Scanning force microscopy observation of the wear track showed that after 400 tracking cycles, the rough surface of the grafted polymer was worn away by the sliding probe. In brittle polymer brushes, coarse slip bands and fractured polymers form as a result of highly localized stress inhomogeneity. The PMBL brushes exhibited stable friction coefficient of about 0.2 after 400 friction cycles, which clearly demonstrates a better wear resistance. Although the slight wear track formed on the brush surface during the friction test, a decreased amount of wear debris and an overall smoother wear track were observed. Sue et al. reported that scratch visibility mainly depends on the yield zone size and fragmentation of the wear surface. This strongly suggests that the PMBL brushes will have great potential for practical scratch resistant applications.¹⁵ Elemental analysis by scanning electron microscopy observation with energy dispersive X-ray detector (SEM-EDX) revealed that the PMBL brush component remained on the wear tracks. Although, the PMBL brush layer was slightly scratched and compressed by sliding probe, the brushes exhibit sufficient toughness to support the applied shear stress due to

**Figure 3.** Variations of friction coefficient with number of friction cycles for (a) PMBL brushes and (b) PMMA brushes at 298 K under nitrogen atmosphere.

the high density and polar interaction. We have previously confirmed that the polymer brush remains in the wear track during the friction test as long as a stable friction coefficient is achieved.^{7,5c} The tribological properties of the spin-coated films were also measured. The spin-coated PMBL films exhibit less wear resistance compared with the corresponding PMBL brushes (Figure S2(a), Supporting Information). The friction coefficient rises immediately at the beginning of the wear test and the polymers are completely scratched away from the wear track. However, it is unclear whether the behavior is due to the substantial weakness and low adhesion force of the spin-coated films or the surface roughness.

In conclusion, we have successfully prepared high-density PMBL brushes through surface initiated controlled radical polymerization. The unique physicochemical characteristics of PMBL brushes were also reported. The useless brittle PMBL form homogeneous thin film and get toughness through graft-density control. This is an example of a resurgent of brittle biobased plastics with the nanostructure control as rigid polymer brushes.

■ ASSOCIATED CONTENT

📄 Supporting Information

Additional figures and experimental details. This material is available free of charge via the Internet at <http://pubs.acs.org>.

■ AUTHOR INFORMATION

Corresponding Author

*E-mail: takahara@cstf.kyushu-u.ac.jp.

Notes

The authors declare no competing financial interest.

■ REFERENCES

- (1) (a) Akkapeddi, M. *Macromolecules* **1979**, *12* (4), 546–551. (b) Akkapeddi, M. *Polymer* **1979**, *20* (10), 1215–1216. (c) Koinuma, H.; Sato, K.; Hirai, H. *Makromol. Chem., Rapid Commun.* **1982**, *3* (5), 311–315.
- (2) (a) Milner, S. T. *Science* **1991**, *251* (4996), 905–914. (b) Zhao, B.; Brittain, W. J. *Prog. Polym. Sci.* **2000**, *25* (5), 677–710.
- (3) (a) Klein, J.; Kumacheva, E.; Mahalu, D.; Perahia, D.; Fetters, L. *Nature* **1994**, *370* (6491), 634–636. (b) Klein, J. *Annu. Rev. Mater. Sci.* **1996**, *26* (1), 581–612. (c) Tadmor, R.; Janik, J.; Klein, J.; Fetters, L. *J. Phys. Rev. Lett.* **2003**, *91* (11), 115503.
- (4) (a) Boyes, S. G.; Granville, A. M.; Baum, M.; Akgun, B.; Mirous, B. K.; Brittain, W. J. *Surf. Sci.* **2004**, *570* (1–2), 1–12. (b) Barbey, R.; Lavanant, L.; Paripovic, D.; Schüwer, N.; Sugnaux, C.; Tugulu, S.; Klok, H.-A. *Chem. Rev.* **2009**, *109* (11), 5437–5527.
- (5) (a) Yamamoto, S.; Ejaz, M.; Tsujii, Y. *Macromolecules* **2000**, *33* (15), 5602–5607. (b) Kobayashi, M.; Terayama, Y.; Hosaka, N.; Kaido, M.; Suzuki, A.; Yamada, N.; Torikai, N.; Ishihara, K.; Takahara, A. *Soft Matter* **2007**, *3* (6), 740–746. (c) Ishikawa, T.; Kobayashi, M.; Takahara, A. *ACS Appl. Mater. Interfaces* **2010**, *2* (4), 1120–1128.
- (6) (a) Matyjaszewski, K.; Xia, J. *Chem. Rev.* **2001**, *101* (9), 2921–2990. (b) Mosnacek, J.; Matyjaszewski, K. *Macromolecules* **2008**, *41* (15), 5509–5511.
- (7) Sakata, H.; Kobayashi, M.; Otsuka, H.; Takahara, A. *Polym. J.* **2005**, *37* (10), 767–775.
- (8) Matsuno, R.; Yamamoto, K.; Otsuka, H.; Takahara, A. *Macromolecules* **2004**, *37* (6), 2203–2209.
- (9) (a) Maoz, R.; Sagiv, J.; Degenhardt, D.; Möhwald, Peter, H. *Supramol. Sci.* **1995**, *2* (1), 9–24. (b) Kojio, K.; Tanaka, K.; Takahara, A.; Kajiyama, T. *Bull. Chem. Soc. Jpn.* **2001**, *74* (8), 1397–1401. (c) Koga, T.; Morita, M.; Ishida, H.; Yakabe, H.; Sasaki, S.; Sakata, O.; Otsuka, H.; Takahara, A. *Langmuir* **2005**, *21* (3), 905–910.

(10) Ishida, H.; Koga, T.; Morita, M.; Otsuka, H.; Takahara, A. *Tribol. Lett.* **2005**, *19* (1), 3–8.

(11) (a) Gao, L.; McCarthy, T. J. *Langmuir* **2006**, *22* (14), 6234–6237. (b) Gao, L.; McCarthy, T. J. *Langmuir* **2007**, *23* (7), 3762–3765.

(12) Owens, D. K.; Wendt, R. C. *J. Appl. Polym. Sci.* **1969**, *13* (8), 1741–1747.

(13) If a circle with radius a (m) is regarded as the contact area between a stainless steel ball and substrate under a normal load P (0.49 N), Hertz's theory affords the following relationship using Young's modulus of stainless and silicon wafer, E_A (1.93×10^{11} Pa), E_B (1.30×10^{11} Pa), and Poisson's ratio ν_A (0.30), ν_B (0.28), respectively: $2/E = (1 - \nu_A^2)/E_A + (1 - \nu_B^2)/E_B$ and $a = ((3/4)(2/E)PR_A)^{1/3}$, where R_A is the curvature radius (5.00×10^{-3} m) of stainless steel ball. The contact area can be calculated by πa^2 .

(14) (a) Yamamoto, S.; Tsujii, Y.; Fukuda, T. *Macromolecules* **2002**, *35* (16), 6077–6079. (b) Tanaka, K.; Kojio, K.; Kimura, R.; Takahara, A.; Kajiyama, T. *Polym. J.* **2003**, *35* (1), 44–49.

(15) Xiang, C.; Sue, H. J.; Chu, J.; Coleman, B. J. *Polym. Sci., Part B: Polym. Phys.* **2001**, *39* (1), 47–59.

(16) Tamai, Y.; Konishi, T.; Einaga, Y.; Fujii, M.; Yamakawa, H. *Macromolecules* **1990**, *23* (18), 4067–4075.